Reduction of Atmospheric Scattering for Remote Sensing Data on the Sea Surface

Sigeru Omatu[+], Hiromu Koda[++] and Tomohiro Yosida[+]

+ Department of Information Science and Intelligent Systems,
Faculty of Engineering, University of Tokushima,
Tokushima, 770, Japan
++ Department of Information Processing, Faculty of Engineering,
Fukuyama University, Fukuyama, 729-02, Japan
Commision No. III

Abstract

The red tide in Seto Inland Sea, Japan affects us serious damages for fishermen and inhabitants in that district. The red tide will appear according to the water quality and whether conditions but it is difficult to measure the data directly because of the rapid change of the conditions and time consuming constraints for measurement by boats. In this case, the remote sensing data analysis is effective since the remote sensing technique enables us to observe the reflectance of the object instantaneouysly and in a wide range. Since reflectance energy is weak and sensitive, we must consider the effect of the path radiance included in the remote sensing data. In this paper, we propose the coorection method of distortion of remote sensing data due to the pass radiance based on both the statisitcal method and physical modeling method. These methods are applied to the remote sensing data observed in summer at the district of Seto Inland Sea in Japan to estimate the mechanism of red tide generation.

1. Introduction

The rapid growth of industry in Japan affected the serious damages for the environmental situation of the air and water quality. One of the damages would be be river or sea water pollution and many rivers or sea bays became overnourished. As a result, the red tide appeared in the sea near bays in Japan in summer and many weak fish were killed. But the mechanism of red tide generation has not been clarified up to now.

In order to consider the cause of the red tide we have applied the remote sensing technique by taking into the consideration that the remote sensing has advantages stated above. But we have found that the data by the multi spectral scanner include the pass radiance and random noise after data processing. Usually, in order to delete the pass radiance the data at the central part of scanning line have been used and the remaining data have been omitted from the data processing. Since these data include a part of information about the object pixcel, it is meaningful to use the data at the remaining part as much as possible. In this paper, we propose an algorithm to correct the pass radiance based on both the regression analysis and the physical modeling approach.

2. Study Area and observation data

The study area is shown in Fig.1 where the numbered points are observation places of water qualities when the remote sensing data are observed. The items

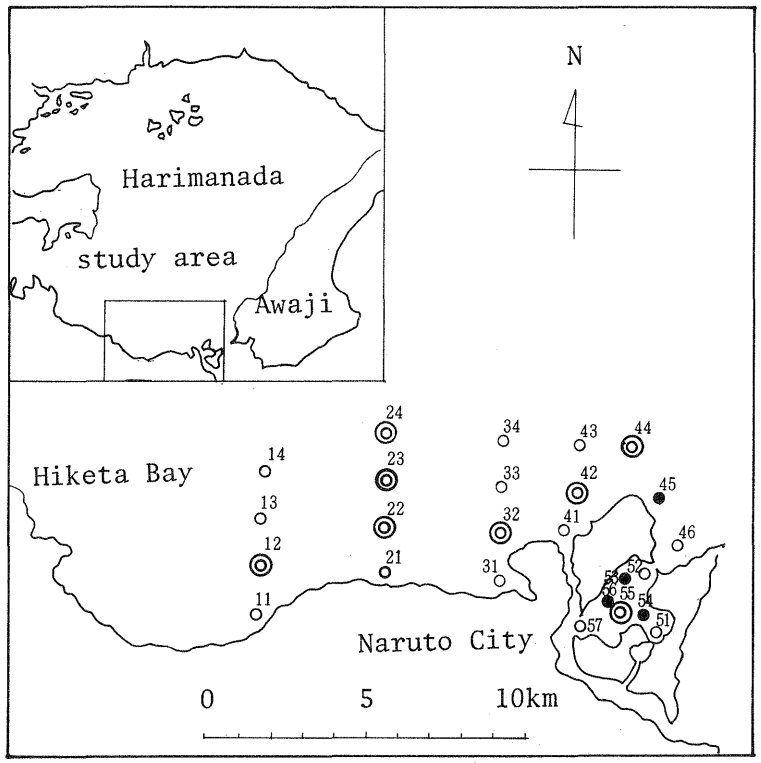

Fig.1. Study area for remote sensing and sea truth data naalysis.

Table 1. MSS specification used in the experiment(unit μm)

Names of MSS		JSCAN-AT-12M	MSS-BG-IA	JSCAN-XM
Used days		July 28, 80	July 24, 81	Aug. 4, 82
Channel Numbers	0	0.25-0.35	0.30-0.35	0.30-0.35
	1	0.35-0.40	0.35-0.40	0.35-0.40
	2	0.40-0.45	0.43-0.45	0.43-0.45
	3	0.45-0.50	0.47-0.49	0.47-0.49
	4	0.50-0.55	0.51-0.53	0.51-0.53
	5	0.55-0.60	0.54-0.56	0.54-0.56
	6	0.60-0.65	0.60-0.65	0.60-0.65
	7	0.65-0.70	0.66-0.68	0.66-0.68
	8	0.70-0.80	*	0.70-0.80
	9	0.80-0.90	0.80-0.90	0.80-0.90
	10	0.90-1.10	*	0.90-1.10
	11	8.00-14.0	10.5-12.5	10.0-12.5
	12	*	4.3-5.5	10.0-12.5
	13	*	2.1-2.4	2.10-2.40

Table 2. Regression equations in 1980 where cor means multiple correlation coefficient and * and ** denote the threshold values of F-test for 1% and 5%, respectively.

items	regression equations	cor.	F
chlorophyl-a	$y=-.35x_3-.03x_3+.63x_7-.8.93$	.99	**
transparency	$y=.24x_3-.31x_5+5.36$	.91	**
SS	$y=-.13x_3+1.7x_5+2.31$	.91	**
salinity	$y=-.01x_3+.04x_5-.05x_7+18.3$	.63	*
sea temperature	$y=.035x_{11}+21.11$		*

Table 3. Regression equations in 1981.

items	regression equations	cor.	F
chlorophyl-a	$y=-.46x_6+.21x_7+24.83$	.93	**
transparency	$y=.60x_6+.10x_7+8.11$	.91	**
SS	$y=-.23x_6+.14x_7+8.51$	.74	*
salinity	$y=-.11x_6+.05x_7+35.57$	.92	**
sea temperature	$y=.09x_{11}+12.13$	.56	*

Table 4. Regression equations in 1982.

items	regression equations	cor.	F
chlorophyl-a	$y=-.02x_5+7.57$	.40	*
SS	$y=.03x_7+.01x_{11}-5.12$	.61	**
T-P	$y=.01x_7-.01$	.51	**

measured at these points are sea temperature, salinity, transparency, COD, DO, chlorophyl-a, SS, T-P, T-N, and water color. The remote sensing data were observed from airborne multi spectral scanner(MSS) whose specifications are shown in Table 1. The remote sensing data were observed in summer three times from 1980 to 1982.

3. Regression analysis

Using the regression analysis for the sea truth data and remote sensing data, we have obtained the regression equations for several observation data. From these regression equations, we can estimate the water qualities in those study area from only the remote sensing data. In Tables 2-4 we show the regression equations in 1980 we can see that the MSS data of channels 3, 5, and 7 are mainly effective to estimate the chlorophyl-a, transparency, SS, and salinity distributions. On the othre hand, for the sea temperature the remote sensing data of channel 11 is effective. Similar results have been obtained for the regression equations in 1981 and 1982.

4. Statistical data correction

During the data processing of the MSS remote sensing data, we have found that the MSS data have been affected heavily by atmospheric scatteing effects. In order to see this, we will pick up the histgram of the MSS levels in the specific area where the observed data by the sea truth are almost equal and there is no object affecting a special effect to produce some biasness in MSS data, for example, a wide range of green grass at one side of the study area. Figs. 2 and 3 show the histgrams of channels 3 and 5, respectively. Fig.4 shows the histgram of channel 11. From these figures, we can see that the remote sesnsing data have some biasness which makes the MSS levels larger near the endpoints of 0 to 10 channels compared with the data at the central part in the scanning lines. But the converse phenomena occurred for the channel 11. Therefore, in order to correct this effect we must make some correction model. From computational viewpoints, we fit quadratic curves for column line levels as follows:

Table 5. Results for quadratic fitting where x ranges from 1 to 268.

channel No.	a	b	c	-b/(2c)
0 ch.	188.2	-1.135	0.004	129.03
1 ch.	148.7	-0.83	0.003	118.57
3 ch.	166.8	-0.943	0.003	131.00
5 ch.	123.0	-0.625	0.002	135.85
7 ch.	120.7	-0.470	0.002	138.29
9 ch.	131.8	-0.300	0.001	149.85
11 ch.	81.8	0.385	-0.001	146.73

$$y = a + bx + cx^2 \qquad (1)$$

where x denotes the column line and y is MSS level. Let Y be the observed MSS data and let M be the average value of column levels. Then the correction algorithm is given by

$$\bar{Y} = k(y - Y) + M \qquad (2)$$

where k is some gain constant and usually it is equal to 1/2. Table 5 shows the regression curve of (1), from which we can see that for the lower channel, that is, for the higher frequency range the quadratic curve becomes shaper and shaper. Furthermore, the coefficient c becomes negative for the channel 11 while the other channels have the positive coefficients, that is, upper convex functions.

5. Atomospheric scattering model

In order to see the reason of distortion of MSS data stated above, we consider the atmospheric scattering model. We assume that the MSS observe three components, that is, the radiance of the object pixel (the reflectance of which is denoted by r), the radiant flux scattered from the sun light, and the radiant flux reflected from the terrain surrounding the object pixel (with average reflectance n). Fig.5 shows these components where L denotes the radiance. The first component is the quantity which reaches MSS after the sun light reflected at the object pixel and it will be decreased since the quantity reflected at the object pixel suffers the absorption and the scattering of the atmosphere. The second component is the quantity which directly reaches MSS after the sun light scattered in the atmosphere. This quantity has nothing to do with the earth surface and it is useless when we want to acquire the information of the earth surface. The third quantity is what is reflected from terrain surounding the object pixel and subsequently scattered to MSS by the atmosphere. The quantity makes the data smooth when we aquire the information of the earth surface.

Based on the single-scattering approximation, that is, an assumption that a photon which underwent scattering either leaves the top of the atmosphere or strikes the surface, J. Otterman et al. proposed the atmospheric model of Landsat[1]. They assume that

1) the atomosphere is horizontally homogeneous,
2) the reflectance of the earth surface is constant,
3) the optical thickness of the atmosphere is small, and
4) the earth surface is the Lambert plane.

But their model does not include any component concerning with the scanner angle. Thus, we propose another model based on their model. Let a_s be the reflectivity observed by the airborne MSS and let F, B, and W be optical thickness of the forward scattering, the backward scattering, and the absorption, respectively. Furthermore, let θ_0 be the solar zenith angle and let $\mu_0 = \cos\theta_0$. When the scanner angle is ϕ, we propose the following scattering model:

$$a_s = r(1 - (B+W)/\mu_0 + 2rB) - r(B+W)/\cos\phi + g(\cos(\theta_0+\phi))b/(2\mu) \qquad (3)$$

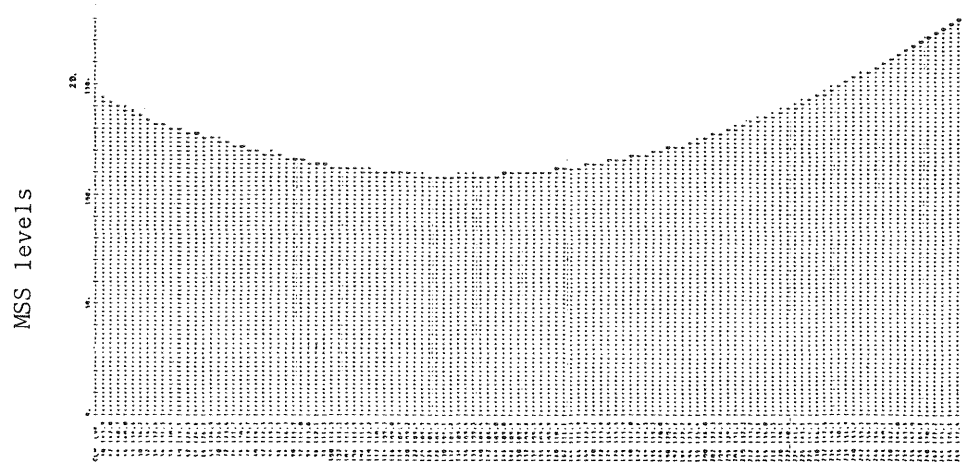

Fig. 2. Column line of the average MSS data for channel 3.

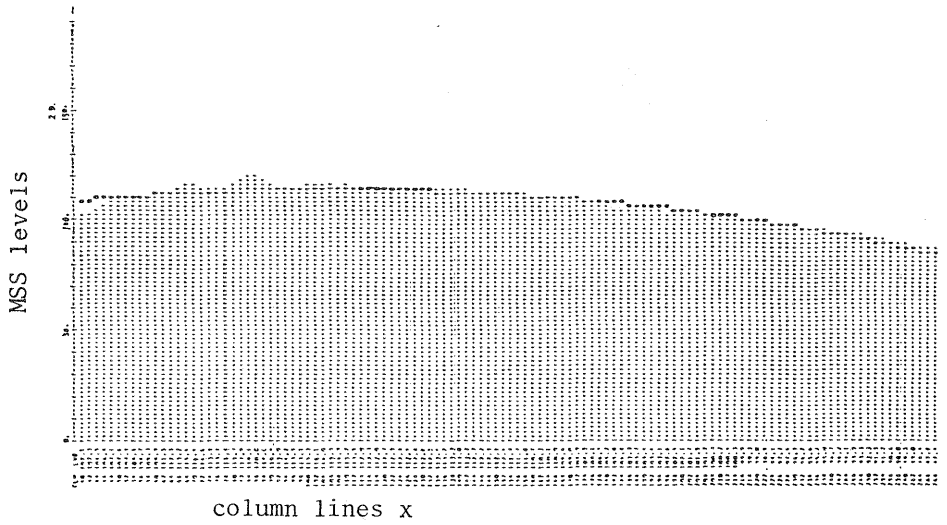

Fig. 3. Column line of the average MSS data for channel 5.

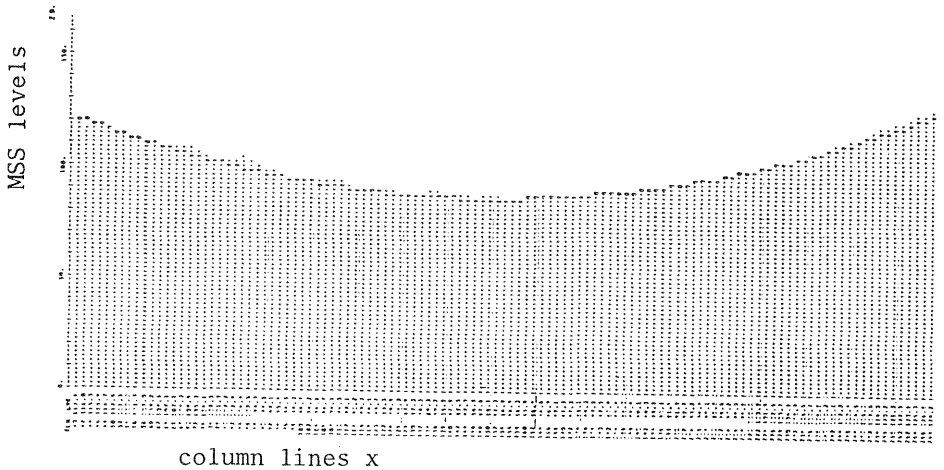

Fig.4. Column line of the average MSS data for channel 11.

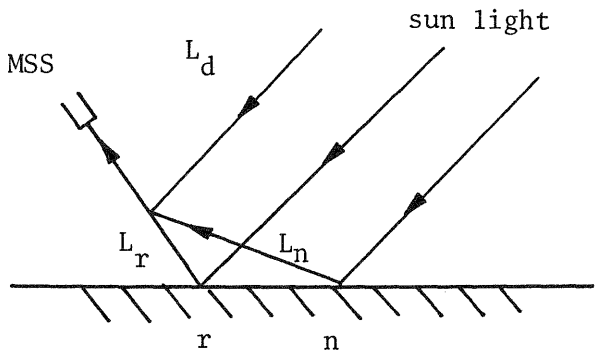

Fig.5. Three components in MSS data.

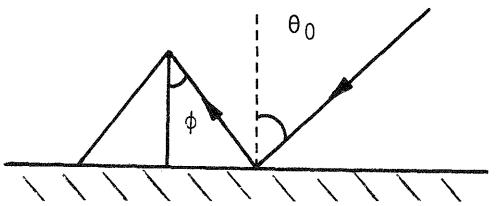

Fig.6. The relation between the MSS angle and the solar zenith angle.

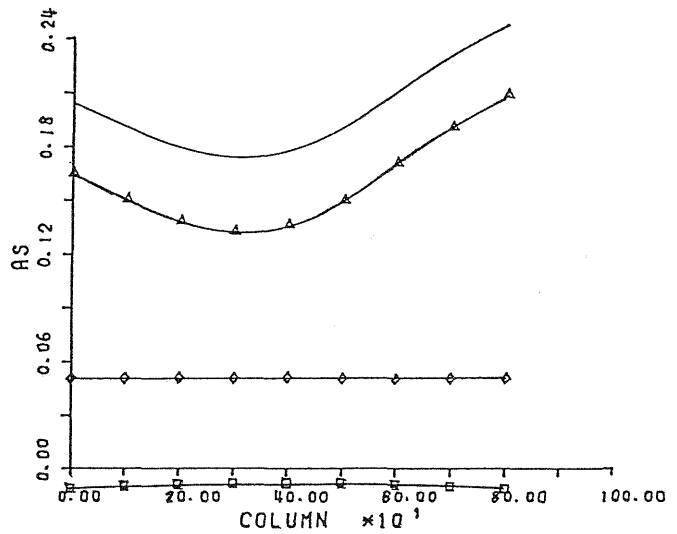

Fig. 7. Results for θ_0 = 80°, B=0.061, and W=0.027

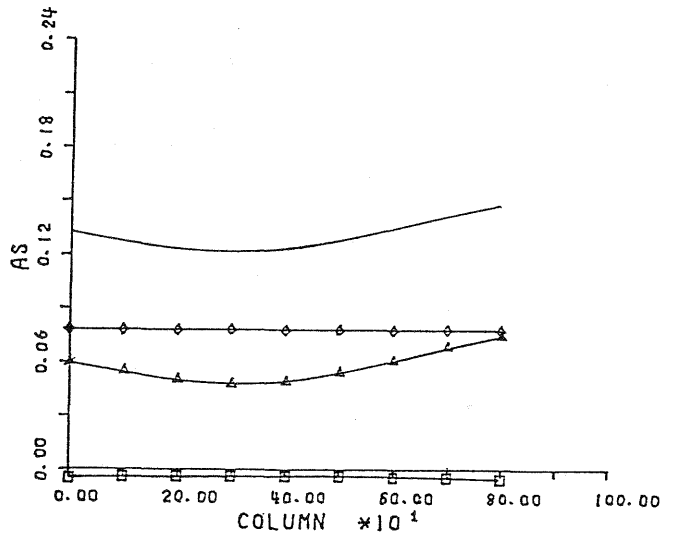

Fig. 8. Results for θ_0 = 80°, B=0.02204, and W=0.017.

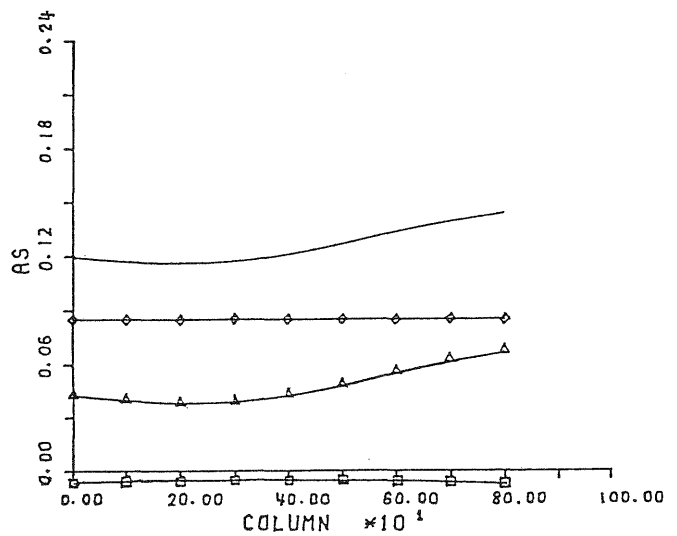

Fig. 9. Results for θ_0 = 80°, B=0.061, and W=0.027.

where g(.) denotes the anisotropy of back scattering to the zenith from the direct beam. Thus, when we think only Rayleigh scattering,

$$g(\mu_0) = 3(1+\mu_0^2)/4. \quad (4)$$

Fig.6 shows the relation between the scanner angle and the simulation results of (3). In Figs. 7-9, —— denotes a_s and —◇—, —□—, and —△— show the first, second, and third term in the right hand side of (3), respectively. The columns of the holizontal axis are from 1 to 802 and column 1 shows $\phi = 40^\circ$ and column 802 shows $\phi = -40^\circ$. From the simulation results, we can see that 1) the result by using (3) looks like quadratic form, the second term does not change so much and its absolute value is small, which means that the quadratic form of the simulation result is affected mainly by the third term, that is, the path radiance, and finally, the central axis movement of the quadratic curve is based on the land area effect where the high reflectivity by trees or grasses exist.

6. Conclusions

In this paper, we have proposed to correct the distortion of the remote sensing data from statistical and physical viewpoints. The result by using the physical model used here conformed to that of the statistical model. Thus, we can use each method independently to delete the pass radiance included in the remote sensing data. By comparing these methods we can see that the statistical method is more flexible than the physical modeling method since the correction parameters can be estimated by using the observed MSS data. But the statistical method cannot offer any physical meaning although the physical modeling method gives us the concrete meaning of the parameters and the correction method. Thje remaining problem is to apply the present method to correct the shadow area by the cloud.

References

[1] J. Otterman and C.J. Robinove, " Effects of the atmosphere on the detection of surface changes from Landsat multi-spectral scanner data", Int. J. Remote Sensing, Vol.2, No.4, pp.351-360, 1981.

[2] S. Omatu, H. Koda, and A. Kikuchi, "Red tide analysis in Harimanada sea area by remote sensing image analysis", Trans. of IEE of Japan, Vol.104, No.11, pp.281-287, 1984.